Evolution in Electrical and Electronic Engineering Vol. 3 No. 2 (2022) 238-245

EEEE

Homepage: http://publisher.uthm.edu.my/periodicals/index.php/eeee
e-ISSN : 2756-8458

Reduction of Cogging Torque in Permanent Magnet Flux Switching Motor

Siti Fatimah Hisham[1], Erwan Sulaiman[1]*

[1]Faculty of Electrical and Electronic Engineering,
Universiti Tun Hussein Onn, Batu Pahat, 86400, MALAYSIA

*Corresponding Author Designation

DOI: https://doi.org/10.30880/eeee.2022.03.02.028
Received 18 July 2022; Accepted 07 September 2022; Available online 30 October 2022

Abstract: A high cogging torque is typically the root cause of unwelcome vibration, improper posture, audible noise, and potentially hazardous operating failures. As a result, this thesis proposes a way of reducing the cogging torque using various methods of three-phase 12S-10P PMFSM. Notching and chamfering are two of the many methods that have been proposed and examined as potential ways to reduce the amount of torque caused by cogging. The values of the cogging torque were derived as a result of the analysis observation. The analysis was simulated using both machines in order to find the differentiation between them and then compare their results to one another in order to determine which one produced the superior result. From its initial value of 4.263Nm, the cogging torque of a 12S-10P PMFSM was found to be lowered using conventional procedures for Chamfering is 0.088Nm and 0.365Nm for Notching. According to the simulation results, the percentage of cogging torque reduced for notching is 12.18% and 71.05% for chamfering.

Keywords: PMFSM, Cogging Torque, Chamfering, Notching

1. Introduction

The permanent magnet flux-switching motor (PMFSM) is one of the stator-PM machines that has gotten a lot of attention since it was first introduced because of its high-power density and torque capacity. The Permanent Magnet Flux Switching Motor (PMFSM) is a novel electric motor design that combines features from the switching reluctance motor (SRM) and the inductor alternator [1]. The PMFSM has a straightforward design and is comprised of a rotor with teeth. The PMFSM consists of a stator part in which the PM winding and the armature winding are carried. Because of the stator's architecture, it is simple to build a cooling system for applications with high speeds [2].

The torque required to overcome the opposing torque caused by the magnetic attractive force between the rotor's magnets and the stator's iron teeth known as cogging torque. The motor's performance suffers because of the cogging torque, which causes unwanted vibration, acoustic noise, dangerous running failures, pitiable speed control, performance degradation and poor position [3].

Corresponding author: erwan@uthm.edu.my

As a result, to lessen the impact, it is very necessary to minimize the effect that high torque pulsations have. To address all of this ineffectiveness, it is essential for Permanent Magnet Motor to have a number of solutions at their disposal to reduce the amount of torque pulsation [4].

Thus, this research proposes a novel structure of a three-phase Permanent Magnet Flux Switching Machine (PMFSM) that employs several techniques including chamfering and notching to reduce the cogging torque.

So, there are three objectives of this research which is the first is to design and observe the performance of 2D 12 slot – 10 pole PMFSM in terms of flux linkage, cogging torque and back electromotive force (emf). The next objective is to minimize the cogging torque of PMFSM by using chamfering and notching. The last objective is to compare the performance of the initial and improved design of the Permanent Magnet Flux Switching Motor.

2. Methodology

In this research, a 12-slot, 10-pole permanent magnet flux switching motor (PMFSM) was designed using J-MAG Designer and tested for its ability to reduce cogging torque using 2D finite element analysis (FEA).

2.1 Design and Analysis Performance of 12S-10P PMFSM

In the Geometry editor, a final diagram of a PMFSM with 12 slots and 10 poles was made by drawing the rotor, stator, permanent magnet, and armature coil part using the region mirror pattern and the region radial pattern. After the drawing is done, the design is linked to the JMAG designer, where the material and conditions are put into place for the motor. Figure 1 shows how the 12S-10P of PMFSM is sketched in the JMAG designer.

After the 4S-8P PMFSM has been designed and the cogging torque, flux linkage, and back-emf have been studied, the first goal of this research had been reached. In no-load research, both the voltage and the current in the windings are removed. Then, we apply load analysis to the motor, changing the armature current from 5Arms/mm^2 to 30Arms/mm^2 to see how the different values affect the motor's torque. The procedure for analyzing the performance of a 4S-8P PMFSM is depicted in Figure 1 and Figure 2.

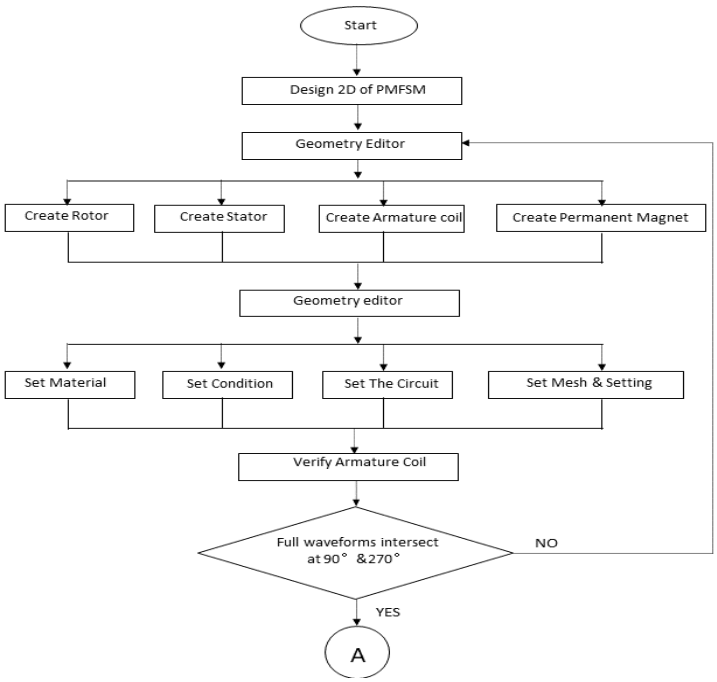

Figure 1: Workflow for design stage PMFSM

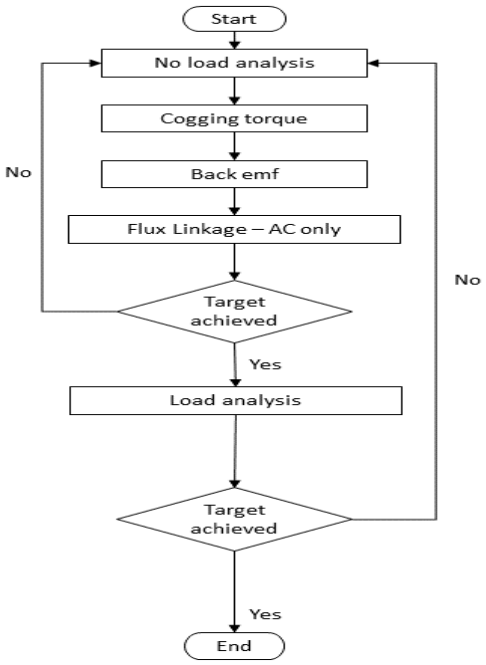

Figure 2: Performance analysis of 12S-10P PMFSM based on 2D-FEA

2.2 Cogging Torque Characteristics

Using the Fourier series and the finite element approach, we can define the cogging torque as the derivative of the output torque. As seen in Eq. (1), the output torque is calculated as the product of the energy and time differentials.

$$P_m = \frac{dW_m}{dt} = T\frac{d\theta}{dt} = Tw \quad \text{Eq.1}$$

Where P_m is the power, dW_m is a differential product of energy, T is the torque output, dθ is the differential mechanical angle and w is the angular velocity [5]. The torque of a motor, which is made up of reluctance torque, alignment torque, and cogging torque, was given by Eq. (2).

$$T = T_R + T_A + T_{cog} \quad \text{Eq.2}$$

$$T_R = \frac{1}{2}i^2\frac{dL}{d\theta} \quad \text{Eq.3}$$

$$T_A = Ni\frac{d\emptyset_g}{d\theta} \quad \text{Eq.4}$$

$$T_{cog} = -\frac{1}{2}(\emptyset_g)^2\frac{dR}{d\theta} \quad \text{Eq.5}$$

Changes in the air gap reluctance cause changes in the cogging torque, which in turn causes changes in the magnetic conductance of the magnets and the stator [6]. These changes cause the EMF harmonics of the magnets and the stator to change. The Fourier series can be used to figure out how the cogging torque changes over time in Eq (6).

$$T_{cog}(\theta_m) = \sum_{n=1}^{\infty} T_n \sin(kN_e\theta_m + \theta_n) \quad \text{Eq.6}$$

Where θ_m, T_n, θ_n, N_e is rotor angular position, amplitude of the n-th harmonic, phase angle of the n-th harmonic and smallest common multiple of rotor pole and stator pole respectively [7].

2.3 Cogging Torque Reduction Technique Performance

This chapter discusses the design studies, performance analysis, optimization procedure, and PMFSM cogging torque reduction technique. The initial testing had to look at how much power is being delivered to the wheels by the motor. The initial performance acts as a benchmark against which the optimization process must either meet or surpass.

Using the cogging torque reduction approach, the motor's cogging torque may be further improved. There are notching and chamfered components in the basic cogging torque technique that make up the technique.

Figure 3 shows the flowchart for the method to reduce the cogging torque. As there are a lot of ways to reduce it, two of those ways were chosen. The chamfering and notching technique is used in the design of a motor that was made after optimization. The curve chamfer was used in this project. The curve chamfer dimension is figured out by taking the curve radius of the chamfer on the tip of the rotor pole. On each rotor pole, the chamfer is added to both ends [7].

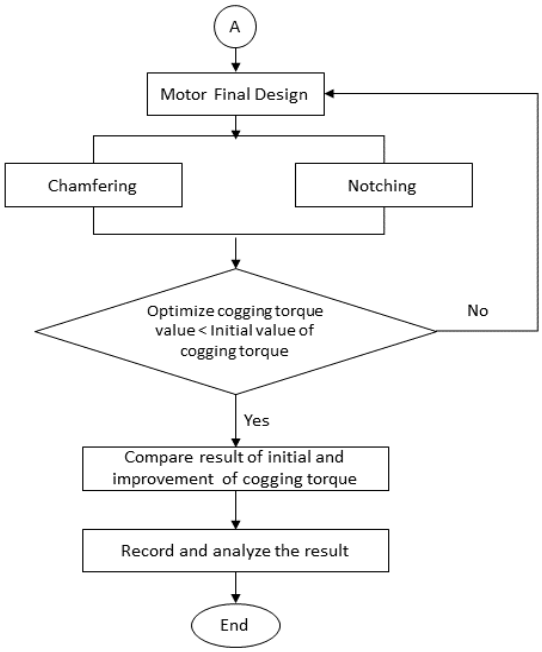

Figure 3: The flowchart on the method to minimize the cogging torque

Next is the notching technique. This research compared the effects of putting an even number of notches on the rotor pole versus an odd number of notches on the rotor pole. It also looked at the effects of putting a notch on the rotor with a variable number of width and height [8]. After simulating both methods, the initial cogging torque and the cogging torque from chamfering and notching had been compared. The next step can be taken if the cogging torque value is going down or is less than the initial value. The outcomes of the initial and improvised design cogging torque, back-emf, and flux linkage results are compared in the following stage. After the improvised design has been implemented, compare the two versions to see whether any differences have occurred.

3. Results and Discussion

With the help of 2D-FEA, the results and analyses of the PMFSM are shown. The first part of the analysis is related to the first goal, which is to design a 12S-10P PMFSM and use it to test the performance of the flux linkage, cogging torque, and back emf. The result is called the initial design. Next, the performance of cogging torque for PMFSM is minimized using traditional methods for reducing cogging torque. Then, the sequential cogging torque reduction technique is used to talk about

the results of reducing the cogging torque. The performance of the 12S-10P PMFSM is judged by how much of the cogging torque is reduced.

3.1 Performance Analysis on 2D Finite Element Analysis

With no-load analysis, the performance correlation for the PMFSM's 12S–10P is attained. The J_a is set to 0 A/mm^2 for no load research to analyze the performance of the flux linkage, cogging torque, and back emf.

3.1.1 Flux Linkage Analysis

PM-produced magnetic flux linkage amplitude for an initial design is accomplished by spinning the rotor at a speed of 1200 r/min while the armature current is set at 0A/mm2. For PMFSM design, the maximum flux value is 0.024 Wb, and the flux linkage of 12S-10P is shown in Figure 4. Due to the flux leakage and cancellation that occurs in the rotor, the flux linkage has a large amplitude, which has an effect on the flux linkage's magnitude.

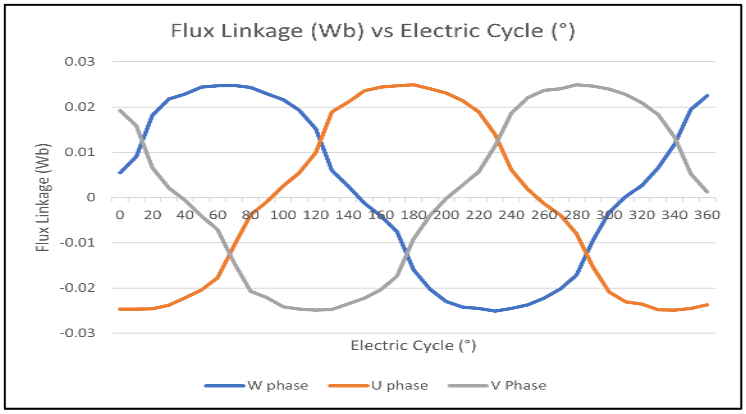

Figure 4: Flux Linkage Analysis Performances

3.1.2 Cogging Torque Analysis

Cogging torque is also called "detent torque," and it causes the motor to vibrate and make noise when it is working. This happens because of how a permanent magnet in the stator and the angle of the rotor work together. By setting the armature current density, Ja, to 0 A/mm2, a permanent magnet delivers the cogging for one electrical cycle. Figure 5 shows the maximum and minimum cogging torque values, which are 4.263 Nm and -4.260 Nm, respectively. The cogging torque value of the motor design is determined by the peak-peak value, which is 8.523Nm, and the cogging torque in 12S-10P of PMFSM can be improved by using the cogging torque reduction technique.

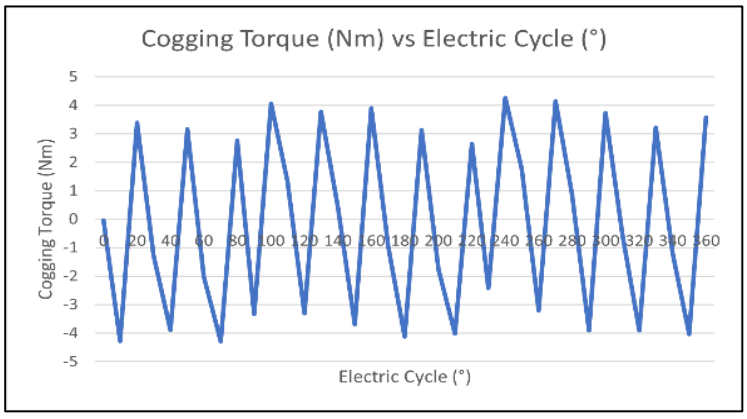

Figure 5: Cogging Torque Analysis Performance

3.1.3 Back EMF Analysis

When the armature current density, J_a, is set to 0 A/mm^2, the analysis of induced voltage may be described as the voltage that rises in electric motors when there is relative movement between the motor armature and the magnetic field of the motor field magnets. Figure 6 depicts the PMFSM back-emf waveform. 12S - 10P PMFSM has a maximum amplitude of 33.1V and a minimum amplitude of -33.1V. The proximity of the rotor pole to the stator pole has resulted in ore flux lines being scattered across the rotor and stator pole. There was less back EMF due to the more aligned flux lines.

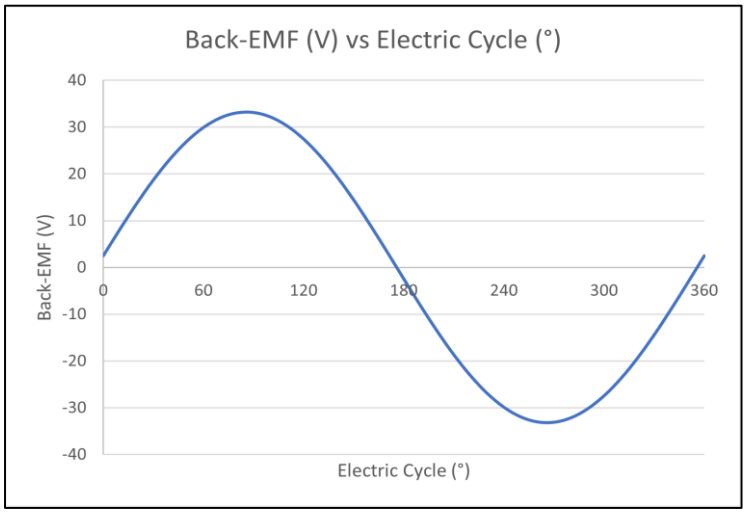

Figure 6: Back-EMF Analysis Performance

3.2 Performance of Cogging Torque Reduction Technique

3.2.1 Notching

With 2D-FEA, the effect of notching technique parameters like notch height on the initial design of cogging torque of 12S-10P PMFSM is studied and shown in Figure 7. The number of notch widths being looked into is 6, which are 1 mm, 0.8 mm, 0.7 mm, 0.5 mm, 0.2 mm, and 0.1 mm. Figure 7 shows that the cogging torque drops from its starting value of 2.127Nm of peak-to-peak cogging torque when the width of the notch increases. When the notch width is 1 mm, which is 0.365 Nm, the cogging torque is the lowest.

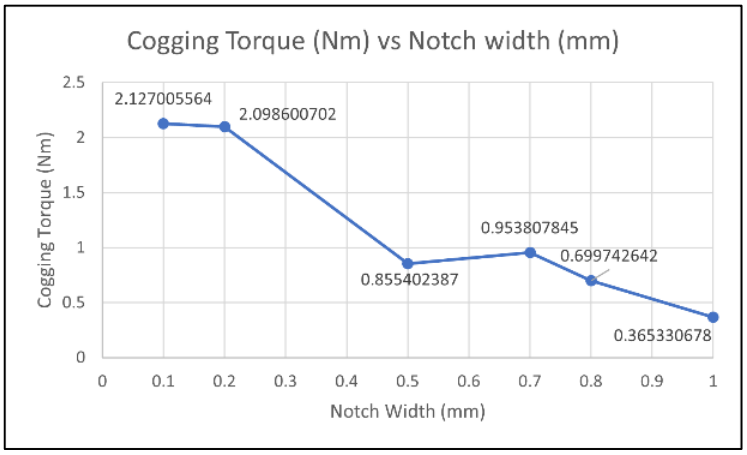

Figure 7: Influence of Notch Width on Cogging Torque of 12S-10P PMFSM

3.2.2 Chamfering

The effect of chamfering technique parameters like the radius of rotor pole tip on the initial design of cogging torque of 12S-10P PMFSM is studied and shown in Figure 8. The radius on tip of the rotor is from 1mm to 5mm. Figure 8 shows the peak-to-peak cogging torque drops from 1.854Nm to 0.088Nm as the number of radius at the rotor tip being chamfer is increasing from 1mm to 5mm.

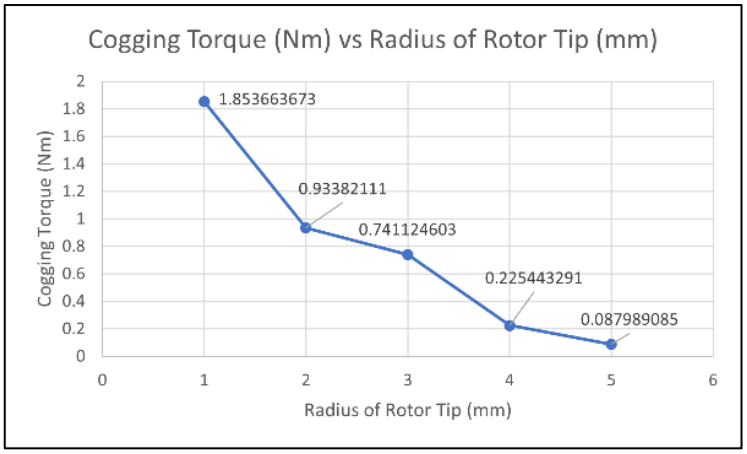

Figure 8: Influence of Various Radius of Rotor Tip on Cogging Torque of 12S-10P PMFSM

4. Conclusion

To summarize, the project's first goal of designing 2D 12S-10P Permanent Magnet Flux Switching Motors (PMFSM) was accomplished because the design of 2D 12S-10P PMFSM was completed. The 12S-10P's flux linkage, cogging torque, and back emf performance are the second goals (PMFSM). The cogging torque effect of 4S-8P PMFSM has been examined and discussed using known and suggested approaches. As a result of the existing rotor-PM arrangement of notching and chamfering, the cogging torque impact of 12S-10P PMFSM appears to be reduced. The cogging torque is reduced from its initial value of 4.263Nm. Rotor chamfering lowered 71.05% of cogging torque to 0.088Nm, whereas rotor notching reduced 12.18% of cogging torque to 0.365Nm. From the result, it can be concluded that chamfering reduces cogging torque more than the other methods.

Acknowledgement

The authors appreciate the assistance provided by the Faculty of Electrical and Electronic Engineering at Universiti Tun Hussein Onn Malaysia.

References

[1] L. I. Jusoh, E. Sulaiman, E. Mbadiwe and H. A. Soomro, "Design of Multi-tooth Permanent Magnet Flux Switching Machine for Electric Bicycle Application," 2019 IEEE 15th International Colloquium on Signal Processing & Its Applications (CSPA), 2019, pp. 174-177, doi: 10.1109/CSPA.2019.8696041.

[2] E. Sulaiman, G. M. Romalan and N. A. Halim, "Skewing and notching configurations for torque pulsation minimization in spoke-type interior permanent magnet motors," 2016 International Conference on Control, Electronics, Renewable Energy and Communications (ICCEREC), 2016, pp. 202-207, doi: 10.1109/ICCEREC.2016.7814984.

[3] Bahrim, Fatihah Shafiqah & Sulaiman, Erwan & Kumar, Rajesh & Jusoh, Laili. (2017). New Cogging Torque Reduction Methods for Permanent Magnet Machine. IOP Conference Series: Materials Science and Engineering. 226. 012127. 10.1088/1757-899X/226/1/012127.

[4] Jenal, Mahyuzie & Sulaiman, Erwan & Kumar, Rajesh. (2016). A New Switched Flux Machine Employing Alternate Circumferential and Radial Flux (AlCiRaF) Permanent Magnet for Light Weight EV. Journal of Magnetics. 21. 537-543. 10.4283/JMAG.2016.21.4.537.

[5] M. Jenal, E. Sulaiman, M. Z. Ahmad, F. Khan and M. F. Omar, "A new alternate circumferential and radial flux (AlCiRaF) permanent magnet flux switching machine for light weight EV," 2016 XXII International Conference on Electrical Machines (ICEM), 2016, pp. 2399-2405, doi: 10.1109/ICELMACH.2016.7732857.

[6] S. M. N. Bin Syed Othman, H. A. Soomro, E. I. Mbadiwe, M. F. Bin Omar and E. b. Sulaiman, "Design and Analysis of Three Phase SegSta 12S-12P Permanent Magnet Flux Switching Machine," 2019 2nd International Conference on Computing, Mathematics and Engineering Technologies (iCoMET), 2019, pp. 1-4, doi: 10.1109/ICOMET.2019.8673491.

[7] N. A. Jafar and E. Sulaiman, "Design analysis of 12S-10P hybrid-excitation flux-switching permanent-magnet machines for hybrid electric vehicle," 2014 IEEE 8th International Power Engineering and Optimization Conference (PEOCO2014), 2014, pp. 308-312, doi: 10.1109/PEOCO.2014.6814445.

[8] F. Khan and E. Sulaiman, "Design optimization and efficiency analysis of 12slot-10pole wound field flux switching machine," 2015 IEEE International Magnetics Conference (INTERMAG), 2015, pp. 1-1, doi: 10.1109/INTMAG.2015.7157489.